Aquacultural Engineering 101 (2023) 102330

Contents lists available at ScienceDirect

Aquacultural Engineering

journal homepage: www.elsevier.com/locate/aque

# Linear modelling of the mass balance and energy demand for a recirculating aquaculture system

Gerard Ayuso-Virgili [a,*], Leila Jafari [b,c], David Lande-Sudall [a], Norbert Lümmen [a]

[a] Department of Mechanical and Marine Engineering, Western Norway University of Applied Sciences, Inndalsveien 28, 5063 Bergen, Norway
[b] Department of Safety, Chemistry and Biomedical Laboratory Sciences, Western Norway University of Applied Sciences, Inndalsveien 28, 5063 Bergen, Norway
[c] Department of Biotechnology and Food Science, Norwegian University of Science and Technology, 7491 Trondheim, Norway

ARTICLE INFO

*Keywords:*
Recirculating aquaculture system
Simulation
Aspen HYSYS
Energy demand
Atlantic salmon (*Salmo salar*)

ABSTRACT

This work seeks to understand the predominant drivers affecting energy demand for a recirculating aquaculture system (RAS) by developing a numerical model in Matlab coupled with Aspen HYSYS and validating against measurement data for a case-study site. 15 weeks of RAS operation were simulated to replicate the grow-out of Atlantic salmon (*Salmo salar*) from 42.5 to 322 g body weight (BW). Data on water quality parameters and the energy demand of the RAS and its equipment were generated. The water treatment loop was automated from Matlab, along with simulation of the fish tanks. Parameters were continuously updated during the quasi-steady dynamic simulation of the RAS and data was stored. Concentrations of oxygen, carbon dioxide, total ammonia nitrogen, total suspended solids and nitrate nitrogen in the fish tanks were recorded for the full 15 week grow-out. The specific energy demand of the RAS was calculated at 9.59 kWh/kg for the full grow-out. In total, 664 MWh were needed for the complete RAS operation. Coupling Matlab and Aspen HYSYS is a viable method for modelling and simulating a RAS. The presented tool can also simulate abrupt changes in the system (such as a power outage) and resume normal operation once power is restored.

## 1. Introduction

Atlantic salmon production in Norway has been steadily increasing over the past decade. In 2019, 350 million salmon smolts were produced compared to the 239 million ten years prior (Fiskeridirektoratet, 2020a, 2020b). In live weight, this is an increase of 58.08 % from 2009 to 2019 (FAO, 2022). At the same time, Recirculating Aquaculture Systems (RAS) have been getting more attention as the favoured land-based aquaculture model. RAS offer operational and environmental advantages compared to Flow Through Systems (FTS) or net pens. Requirements of a freshwater source are much lower in a RAS since most of the water is recirculated and treated, thus limiting emissions in effluent water. The tight control that RAS offer on water quality requires a range of equipment to be installed. The resulting high capital expenditure is one of the challenges for RAS sustainability, but this can be mitigated by large-scale and intensive production (Dalsgaard et al., 2013).

The necessity of such a range of equipment for controlling water quality makes RAS an energy intensive aquaculture practice. Compared to other aquaculture systems, RAS is the most energy intensive method, per mass of fish produced. In a Life Cycle Assessment (LCA), RAS energy demand was 1.4–1.8 times higher than FTS (d'Orbcastel et al., 2009). Another comparative LCA showed the specific energy demand for mass unit of produced fish of FTS to be 2.55 kWh/kg while RAS was several times higher at 19.6 kWh/kg (Samuel-Fitwi et al., 2013). Even though RAS are clearly the most energy intensive, both measured and estimated energy demand show a wide range of values. Reported and estimated energy demand of a RAS in the literature is 3–81.48 kWh/kg (Badiola et al., 2018, 2017; Bergheim and Nilsen, 2015; d'Orbcastel et al., 2009; Hilmarsen et al., 2018; Yogev et al., 2017; Yogev and Gross, 2019).

The disparity in the reported specific energy demand of a RAS might be caused by different RAS topologies and combinations of water treatment components. Investigating how energy demanding these components are can give a better picture of the impact they have on the total RAS energy demand. Since RAS are seldom operated with a constant and controlled biomass, the variability in energy demand of all RAS components also needs to be studied for the duration of the fish grow-out.

RAS modelling and simulation also has been at the center of other studies. Ernst et al. (2000) developed a software for aquaculture process design, management, and simulation. In Wik et al. (2009), a RAS was dynamically simulated with special detail on moving bed biofilm

* Corresponding author.
*E-mail address:* Gerard.Ayuso.Virgili@hvl.no (G. Ayuso-Virgili).

https://doi.org/10.1016/j.aquaeng.2023.102330
Received 29 October 2022; Received in revised form 14 March 2023; Accepted 15 March 2023
Available online 17 March 2023

**Nomenclature**

*Acronyms and variables*

| | |
|---|---|
| RAS | Recirculating Aquaculture System(s) |
| FTS | Flow Through System(s) |
| LCA | Life Cycle Assessment |
| SGR | Specific Growth Rate (%/day) |
| FCR | Feed Conversion Ratio ($kg_{feed}/kg_{fish\ weight\ gain}$) |
| BW | Body Weight (g or kg) |
| DO | Dissolved oxygen (mg/L or %saturation) |
| $CO_2$ | Dissolved carbon dioxide (mg/L) |
| TSS | Total suspended solids (mg/L) |
| TAN | Total ammonia nitrogen (mg/L) |
| $NO_3$-N | Nitrate nitrogen (mg/L) |
| $C$ | Concentration (mg/L) |
| $Q$ | Recirculating water flow (L/h) |
| $\dot{m}$ | Mass flow (mg/h or kg/h) |
| $m$ | Mass (kg) |
| $V_{FT}$ | Fish tank volume ($m^3$) |
| $t$ | Time (h) |
| %TSS | Percentage of TSS removed in drum filter (%) |
| %TAN | Percentage of TAN conversion in the biofilter (%) |
| %Feed | Daily feed ratio (%/day) |
| $r$ | Metabolite production rate (mg/(kg min)) |
| MW | Molecular weight (g/mol) |
| RQ | Respiratory quotient ($mol_{CO_2}/mol_{O_2}$) |
| $a_{TSS}$ | Fraction of TSS in feed ($kg_{TSS}/kg_{feed}$) |

*Subindexes*

| | |
|---|---|
| FT | In the fish tanks |
| FT in | Fish tanks inlet |
| FT out | Fish tanks outlet |
| gen | Metabolite generation |
| Filtered TSS | Drum filter filtrate outlet |
| DF in | Drum filter inlet |
| BF in | Biofilter inlet |
| BF out | Biofilter outlet |
| Pure $O_2$ | Oxygen injected in the oxygen cones |
| OC | Oxygen cones |
| PS | Pump sump |
| BM | Biomass in the fish tanks |

reactors to predict water quality after treatment. Karimanzira et al. (2016) modelled an aquaponic system to simulate RAS effluent water use for crop growth using VBA Excel. Varga et al. (2020) used RAS experimental data to develop a RAS simulator with multiple growth stages. In Tanveer et al. (2020), component material balances for several metabolites were implemented in a dynamic simulation to calculate fish growth and water quality. Kamali et al. (2022) built a RAS model to predict wastewater conditions and fish welfare under different RAS management strategies.

In this study a RAS was modelled, validated, and simulated against an existing RAS whose operators (ERKO Settefisk) and manufacturers (Nofitech) have collaborated by sharing essential data. The focus is not only the correct prediction of water quality parameters, but to estimate the energy demand of the RAS and its main components. The same RAS operation was followed over one production cycle and part of the data on water quality was used for the modelling. The efficiency of the mechanical filter, biofilter, aerator and the metabolite generation models used in the simulated fish tanks in this study were all fitted to experimental data. Since the presented model is semi-empirical, some of the presented equations are only valid under the specific conditions of this case study. Data on measured water quality and analyses is in preparation for a separate peer-reviewed publication.

The proposed hybrid model in Matlab and Aspen HYSYS simulates the grow-out stage of Atlantic salmon post-smolts for a period of 15 weeks, until they are ready to be sent to net pens. Energy demand of all equipment and water quality parameters in the fish tanks are calculated for the grow-out stage. To the authors knowledge, Aspen HYSYS was used for the first time to model and validate the RAS water treatment loop.

Adjusting the recirculating water flow of the main water treatment loop is proposed as an alternative operation schedule to reduce energy demand. All water quality parameters are allowed to remain within certain limits to ensure fish welfare. Water quality in the fish tanks is leveraged within these limits to allow for lower water recirculating flows. Water recirculating flow is increased accordingly with fish growth to prevent water quality parameters to surpass the set limits.

This manuscript is organized in five sections: Section 1 offers a perspective of the current situation of RAS energy demand and the aim with this work. The details on how the modelling and validation of the RAS was performed, and which tools were used are laid out in Section 2. Section 3 contains specific energy demand figures for all RAS components and water quality parameters in the fish tanks for the complete grow out. The results are evaluated and compared to literature in Section 4. Final remarks and key points are summarized in Section 5.

## 2. Methods

Weekly access to a RAS facility (ERKO Settefisk) was offered to the project partners in this work. Water samples were taken from different sampling points along the water treatment loop. Operational parameters such as fish weight, feed fed, or water temperature were noted, and the recirculated water flow was measured. Afterwards, water samples were analysed for a series of different parameters. Water measurements of interest for this article were dissolved oxygen (DO), dissolved carbon dioxide ($CO_2$), total suspended solids (TSS) and total ammonia nitrogen (TAN).

### 2.1. RAS modelling

Two different software programs were used for the simulation of the complete RAS model; Aspen HYSYS V10, and Matlab R2021a. The choice of splitting the RAS model between two programs, instead of building the entire RAS model in one, is the following: Aspen HYSYS has a limited dynamic simulation interface with little flexibility for modifications. The dynamic simulation tool is more focused on process control and operational stability. HYSYS requires a full modelling of a control system for numerous process variables and the tuning of all controllers before dynamic simulation can be performed. Additionally, there is no built-in function for accessing and exporting transient data from a dynamic simulation in the user interface, which makes the data acquisition for obtaining results inconvenient. This discouraged the option of a complete dynamic model in Aspen HYSYS. However, Aspen HYSYS has proven to be very capable when dealing with phase equilibria and mass transfer processes. This makes it an excellent choice for a steady state simulation of the water treatment loop due to its accuracy. To complete the RAS, the fish tanks were simulated dynamically in Matlab. The water treatment loop could also be modelled in Matlab alongside the fish tanks, but at a great time cost and added complexity to match the precision of Aspen HYSYS. The proposed hybrid solution combines both the flexibility of Matlab with the simplicity of using Aspen HYSYS for solving material and energy balances, and multiphase chemical component interaction.

In order to calculate the water conditions of the fish tank inlet flows from a given fish tank outlet conditions, Aspen HYSYS was used to solve the water treatment loop. The loop started with the fish tank outlet (see Fig. 1) and the recirculated water was treated to generate the clean water flow into the fish tanks (see Fig. 2). After this is done for each iteration, all component material flows are imported to Matlab. In the Matlab script, an algorithm (see Fig. 3) solves the component material balances and recalculates the water conditions in the fish tanks. When both fish tank outlet and inlet component mass flows are known, the accumulation $(dC_{FT}/dt)_i$ (mg/(L h)) of each component is calculated for that iteration using Eq. (1).

$$(dC_{FT}/dt)_i = \left(Q\left(C_{i,FTin} - C_{i,FT\ out}\right) + \dot{m}_{gen}\right)/V_{FT} \tag{1}$$

Where, $Q$ (L/h) is the recirculating water flow, $C_{i,FT\ in}$ (mg/L) is the metabolite concentration at the fish tank inlet, $C_{i,FT\ out}$ (mg/L) is the metabolite concentration at the fish tank outlet, $\dot{m}_{gen}$ (mg/h) is the metabolite generation in the fish tanks, and $V_{FT}$ (L) is the fish tank volume.

The fish tank outlet component concentrations $C_{i+1,FT\ out}$ (mg/L) are then calculated for the next iteration, integrating numerically using Eq. (2).

$$C_{i+1,FT\ out} = C_{i,FT\ out} + (dC_{FT}/dt)_i \cdot \Delta t \tag{2}$$

Where, $\Delta t$ (h) is the time interval between iterations.

Since the recirculating water flow is known and constant ($Q = 1.44 \cdot 10^6$ L/h), component mass flows are also calculated. A comparatively small water exchange is present in the RAS; an overflow of 80 L/min for each fish tank is specified. The necessary additional (fresh)water flow to compensate for all system water losses is calculated on each iteration. All new component mass flows are exported to HYSYS and updated on their corresponding so-called material stream at the start of the water treatment cycle. HYSYS calculates the fish tank inlet flows, which are assessed before they are imported into Matlab. This assessment is performed to prevent the use of inaccurate data from an incorrectly solved water treatment loop (i.e., unsolved material streams or negative flows). Under such scenario, the simulation would stop, and a warning message would be issued. The cycle is repeated for a simulated time of 8 h to ensure convergence is reached. This equates to 48 iterations using a time interval of 10 min between iterations. Every new simulated week, the increase in biomass was accounted for and all dependant parameters were adjusted accordingly (e.g., daily feed mass and metabolite generation rates) as depicted in Fig. 3. Then a new set of 8 h were simulated for that new week with its new set of conditions. In the end, all weeks during the grow-out stage were simulated for 8 h each. For every week, all operational conditions, water quality parameters and energy demand were obtained after convergence. These were used as the representative estimate of the whole week's performance.

The reason 8 h was selected is partly arbitrary and mainly to ensure convergence is reached for each simulated week. Diurnal variations in time-depending parameters were not studied due to the continuously even RAS operation throughout the day. All fish were exposed to a photoperiod of 24 h light and lamps in the fish tanks were always on. Also, fish were continuously fed for 24 h a day.

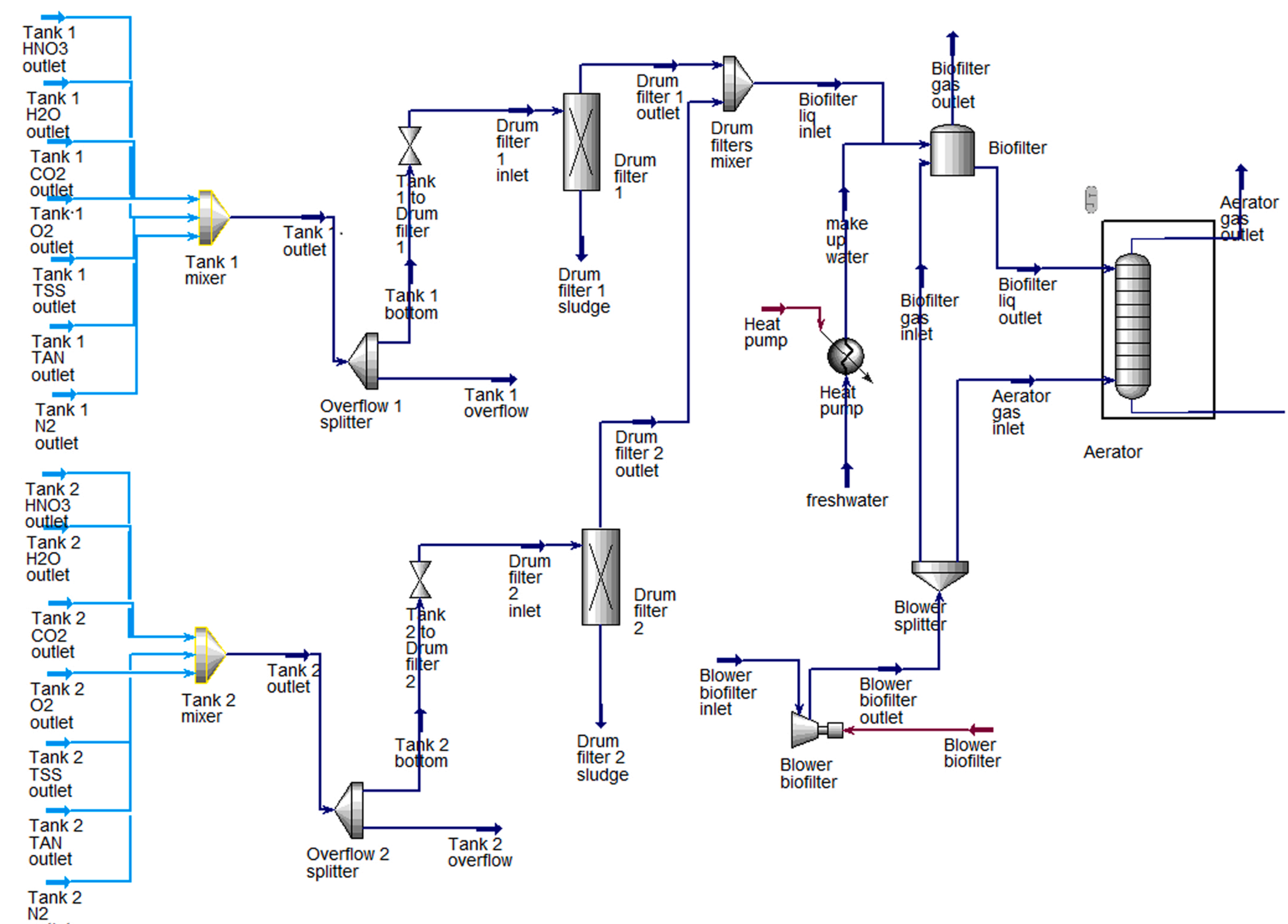


**Fig. 1.** Flowsheet diagram of the RAS model as seen in the Aspen HYSYS user interface. (Part 1).

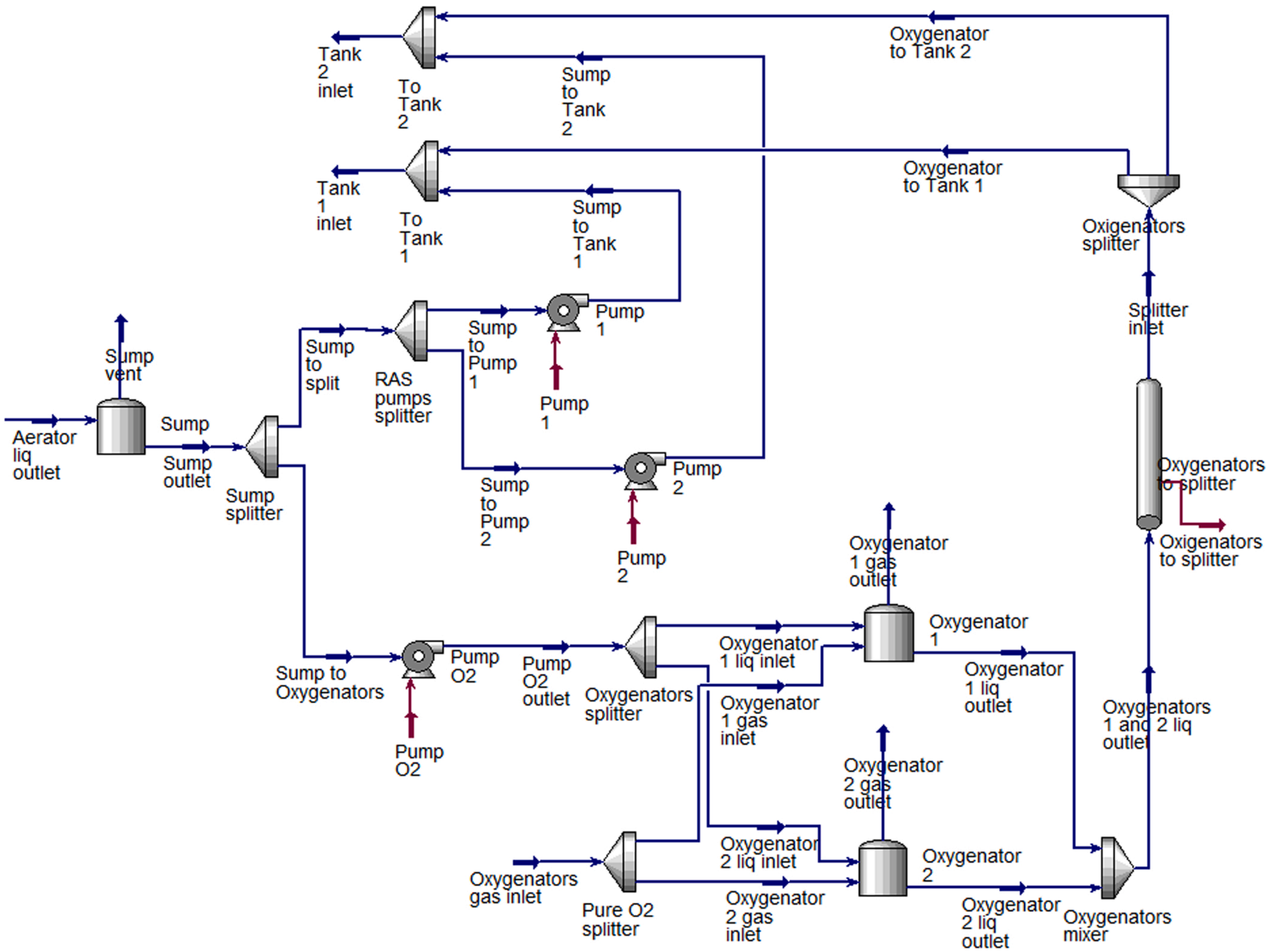


**Fig. 2.** Flowsheet diagram of the RAS model as seen in the Aspen HYSYS user interface. (Part 2).

Since a set of important parameters changed every simulated week (e.g., biomass and metabolite generation rates) a correction was needed between simulated weeks. At the start of a new simulated week, an initial estimation was performed to update the Aspen HYSYS model which still contained the prior week conditions and results. The new week's fish tank outlet conditions were brought closer to their steady state values. For this, Eq. (1) was used under a steady state assumption as shown in Eq. (3) to calculate a first estimate of the new mass flows $\dot{m}_{\mathrm{FT\ out}}$ (mg/h) for each component at the fish tank outlet. This is done once per new simulated week as a new $\dot{m}_{\mathrm{gen}}$ is introduced.

$$\dot{m}_{\mathrm{FT\ out}} = QC_{\mathrm{FT\ in}} + \dot{m}_{\mathrm{gen}} \tag{3}$$

Matlab was also used to automate the water treatment loop in Aspen HYSYS. Certain parameters were calculated and regulated throughout the simulation (e.g., make-up water flow, recirculated water flow redirected to the oxygen cones and necessary oxygen to be injected in the oxygen cones). All data of interest (e.g., energy demand of various equipment and component concentrations in the fish tanks) was continuously imported and stored from HYSYS.

### 2.1.1. *Water treatment loop*

A total of six different chemical species plus a hypothetical solid component (i.e., total suspended solids, TSS) were included in the Aspen HYSYS model. These are nitric acid ($HNO_3$), water ($H_2O$), carbon dioxide ($CO_2$), oxygen ($O_2$), ammonia ($NH_3$) and nitrogen ($N_2$). Each one of these components are given a material stream at the start of the water treatment loop in Fig. 1. They contain the mass flows of all simulated components in the fish tank outlet. These streams are continuously updated by Matlab on each iteration of the simulation. They are assembled in one fish tank outlet flow that goes on through a water treatment cycle. The main water treatment units consist of two drum filters, a biofilter, an aerator (Fig. 1) and two oxygenators (Fig. 2).

The first step is mechanical filtration. A drum filter holds back part of the particulate material in the water and TSS is reduced. The efficiency of the drum filters was found to be 41.7 % from experimental data. This TSS removal efficiency was specified in the model in Aspen HYSYS where the net mass flow of TSS in the filtered water flow, $\dot{m}_{i,\mathrm{filtered\ TSS}}$ (mg/h), is calculated according to Eq. (4).

$$\dot{m}_{i,\mathrm{filtered\ TSS}} = \left(\%\mathrm{TSS}\cdot\dot{m}_{i,\mathrm{DF\ in,TSS}}\right)/100 \tag{4}$$

Where, $\dot{m}_{i,\mathrm{DF\ in,TSS}}$ (mg/h) is the net mass flow of TSS at the drum filter inlet, and %TSS (%) is the percentage of TSS removed in the drum filter.

There is one drum filter for each fish tank in the RAS, all connected in parallel. After the mechanical filtration, both water recirculating flows are combined. The next step is the nitrification of TAN into a less toxic nitrogen species in the biofilter. It was assumed that all TAN is converted into nitrite anion as represented in the chemical reaction in Eq. (5).

$$NH_3 + 2O_2 \rightarrow HNO_3 + H_2O \tag{5}$$

The overall TAN conversion of 45.3 % was calculated from experimental data and implemented in the simulated biofilter. The amount of unreacted TAN in the biofilter outlet $\dot{m}_{i,\mathrm{BF\ out,TAN}}$ (mg/h) is expressed in

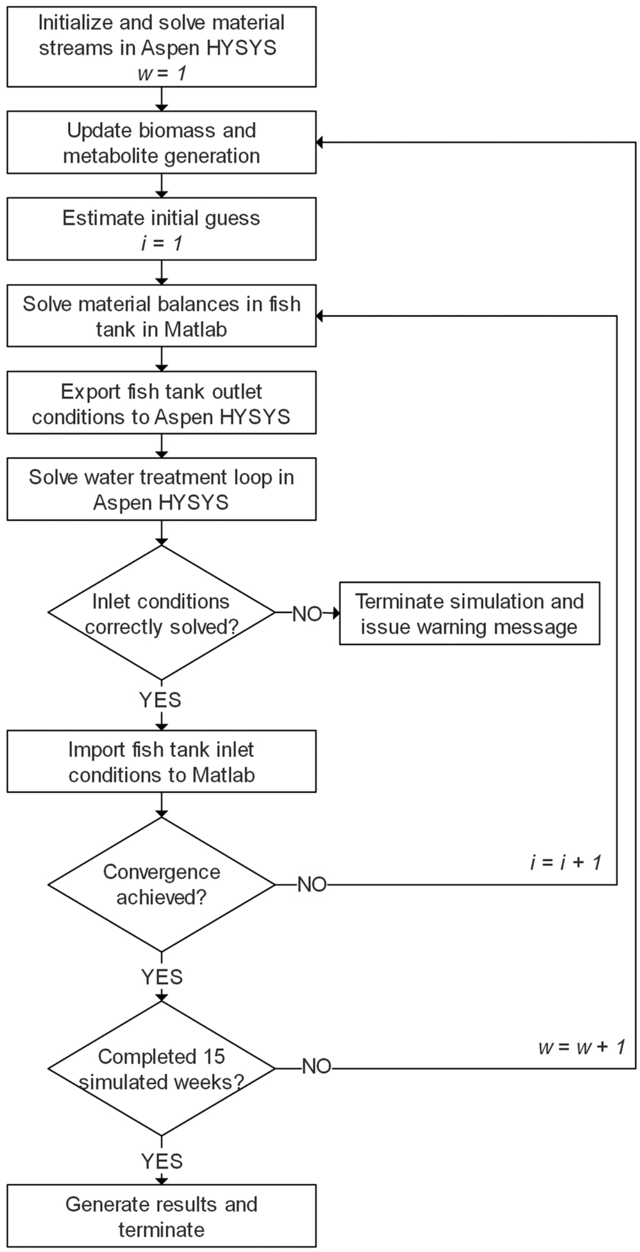


**Fig. 3.** Schematic diagram showing the process and decision-making within the numerical algorithm, as implemented in Matlab.

Eq. (6).

$$\dot{m}_{i,\mathrm{BF\ out,TAN}} = (1 - \%\mathrm{TAN}/100)\cdot \dot{m}_{i,\mathrm{BF\ in,TAN}} \quad (6)$$

Where, $\dot{m}_{i,\mathrm{BF\ in,TAN}}$ (mg/h) is the net mass flow of TAN at the biofilter inlet, and %TAN (%) is the TAN reaction conversion percentage in the biofilter.

Air is sent through the biofilter to ensure aerobic conditions for the nitrification step are kept. High concentrations of DO are important to allow for higher TAN removal rates (Rusten et al., 2006). The effect this airflow has on carbon dioxide stripped is not measured and, instead, an overall carbon dioxide stripping efficiency is calculated between the biofilter inlet and the aerator outlet. This efficiency is implemented in the simulated aerator while no measure on the carbon dioxide stripped in the biofilter is made. Freshwater is added in the biofilter to make up for water losses and water drained through the fish tank overflows. These are the main sources of water exchange in the system with 0.3 % of the recirculating flow being replaced with freshwater which equates to less than 7 % daily water exchange.

The biofilter is followed by the aerator where carbon dioxide is stripped, and water is partly oxygenated. Overall removed carbon dioxide $\%CO_2$ (%) was measured to be 57 %. The efficiency of the aerator was then adjusted so that $CO_2$ in the aerator outlet matched the experimental measurements compared to the biofilter inlet.

After the biofilter, water is sent to a sump where the flow is split in two. Most of the water is pumped through the main recirculating pumps (Pumps 1 and 2 in Fig. 2) back to the fish tanks. A fraction is sent to the oxygen cones for oxygenation before returning to the fish tanks. Pure oxygen pressurized at a maximum of 4 barg is used to reach higher saturation levels of DO and reduce water flow requirements in the oxygen cones.

The water flow redirected to the oxygen cones is controlled to adjust a desired DO level of 9.5 mg/L in the fish tanks. This value was close to measurements done on several weeks throughout the grow-out period.

Eq. (7) is used to predict how much pure oxygen $\dot{m}_{\mathrm{pureO_2}}$ (mg/h) needs to be sent to the fish tanks in order to maintain this DO level.

$$\dot{m}_{\mathrm{pureO_2}} = QC_{\mathrm{FT,O_2}} - \dot{m}_{\mathrm{gen,O_2}} \quad (7)$$

Where, $C_{\mathrm{FT,O_2}}$ (mg/L) is the desired DO level in the fish tanks, and $\dot{m}_{\mathrm{gen,O_2}}$ (mg/h) is the oxygen generation in the fish tanks.

The necessary water flow $Q_{\mathrm{OC}}$ (L/h) that is to be oxygenated is calculated in Eq. (8).

$$Q_{\mathrm{OC}} = \left(2\dot{m}_{\mathrm{pureO_2}} - \dot{m}_{\mathrm{PS,O_2}}\right) / \left(C_{\mathrm{OC,O_2}} - C_{\mathrm{PS,O_2}}\right) \quad (8)$$

Where, $\dot{m}_{\mathrm{PS,O_2}}$ (mg/h) is the net oxygen mass flow in the pump sump, $C_{\mathrm{OC,O_2}}$ (mg/L) is the concentration of oxygen after the oxygen cones, and $C_{\mathrm{PS,O_2}}$ (mg/L) is the concentration of oxygen after the pump sump.

In the case of very low oxygen consumption in the fish tanks (i.e., at the start of grow-out, with low biomass) DO in the pump sump is enough to keep the DO in the fish tanks at the desired level. In these instances, Eq. (8) returns a value for $Q_{\mathrm{OC}}$ (L/h) lower than zero. When this happens, the obtained negative volumetric flow is ignored, and all water is sent to the main recirculating pumps.

### 2.1.2. *Fish tanks*

Matlab was used for the mathematical modelling of the fish tanks. All parameters were validated from experimental measurements and analysis from the real studied RAS.

*2.1.2.1. Specific growth rate (SGR).* Fish growth throughout the grow-out stage was modelled assuming a constant specific growth rate (SGR). This was first calculated using Eq. (9) from experimental measurements between the start and end of fish grow-out.

$$\mathrm{SGR} = \left(\ln(m_{\mathrm{BW\ end}}) - \ln(m_{\mathrm{BW\ start}})\right)\cdot 100 / (t_{\mathrm{end}} - t_{\mathrm{start}}) \quad (9)$$

Where, $m_{\mathrm{BW\ end}}$ (g) is the average fish body weight at end of the grow-out, $m_{\mathrm{BW\ start}}$ (g) is the average fish body weight at start of the grow-out, and $t_{\mathrm{end}} - t_{\mathrm{start}}$ (days) is the number of days the fish grow-out lasted.

The SGR was found to be 1.93 %/day. Applying the experimentally found SGR in the simulation, biomass $m_{w+1,\mathrm{BM}}$ (kg) and $(\mathrm{BW})_{w+1}$ (g) could be calculated each consecutive simulated week using Eqs. (10) and (11).

$$m_{w+1,\mathrm{BM}} = m_{w,\mathrm{BM}}\exp(7\cdot \mathrm{SGR}/100) \quad (10)$$

Where, $m_{w,\mathrm{BM}}$ (kg) is the fish biomass in a fish tank in the current simulated week $w$.

$$(\mathrm{BW})_{w+1} = (\mathrm{BW})_{w}\exp(7\cdot \mathrm{SGR}/100) \quad (11)$$

Where, $(\mathrm{BW})_w$ (g) is the fish body weight in the current simulated week $w$.

*2.1.2.2. Feed.* The feed ratio was constant for the simulated grow-out stage. In the real RAS, feed was adjusted according to satiation. Feeding was reduced right before the end to slow down metabolite generation in water as fish were exported to sea cages. In the simulation, the daily feed ratio was kept at 1.54 %/day. The hourly feed mass $\dot{m}_{w,\mathrm{Feed}}$ (kg/h) was calculated accordingly using Eq. (12).

$$\dot{m}_{w,\mathrm{Feed}} = \%\mathrm{Feed}\cdot m_{w,\mathrm{BM}}/2400 \tag{12}$$

Where, %Feed (%/day) is the daily feed ratio.

*2.1.2.3. Metabolite generation.* Metabolite excretion and consumption was modelled using data from experimental measurements of water samples before and after the fish tanks. The considered metabolites are $CO_2$, DO, TAN and TSS.

*2.1.2.3.1. Carbon dioxide.* Carbon dioxide production rate was found to be 5.276 mg/(kg min). The increase in carbon dioxide excretion with fish growth was accounted for. Eq. (13) was used to calculate the net carbon dioxide mass flow $\dot{m}_{w,\mathrm{gen},CO_2}$ (mg/h) produced in the fish tanks.

$$\dot{m}_{w,\mathrm{gen},CO_2} = 60 r_{CO_2} m_{w,\mathrm{BM}} \tag{13}$$

Where, $r_{CO_2}$ (mg/(kg min)) is the carbon dioxide production rate.

*2.1.2.3.2. Oxygen.* Consumption of oxygen was not modelled based on measurements but derived from the carbon dioxide production rate. The relationship between oxygen and carbon dioxide in fish respiration can be established with the respiratory quotient (RQ). It is a commonly used method for calculating carbon dioxide production from measured oxygen consumption and vice-versa. RQ can be calculated using the model presented in Sanni and Forsberg (1996). The necessary inputs in the model are the proportion of fat, protein, and carbohydrates in fish feed. For simplicity, RQ can also be assumed constant. A RQ value of 0.8 $\mathrm{mol}_{CO_2}/\mathrm{mol}_{O_2}$ was measured for satiated Atlantic salmon in Forsberg (1997). When fish were underfed, the quotient decreased. It reached a lowest value of 0.7 $\mathrm{mol}_{CO_2}/\mathrm{mol}_{O_2}$ when fish were starved (Forsberg, 1997). In this study, a RQ of 0.8 $\mathrm{mol}_{CO_2}/\mathrm{mol}_{O_2}$ was assumed, following the recommendation by Thorarensen and Farrell (2011) for Atlantic salmon feed composition, and the oxygen consumption rate $r_{O_2}$ (mg/(kg min)) was calculated using Eq. (14).

$$r_{O_2} = r_{CO_2}\cdot \mathrm{MW}_{O_2}/(\mathrm{MW}_{CO_2}\cdot \mathrm{RQ}) \tag{14}$$

Where, $\mathrm{MW}_{O_2}$ (g/mol) is the molar weight of oxygen, $\mathrm{MW}_{CO_2}$ (g/mol) is the molar weight of carbon dioxide, and RQ ($\mathrm{mol}_{CO_2}/\mathrm{mol}_{O_2}$) is the respiratory quotient. The rate of oxygen respirated was 4.790 mg/(kg min).

Eq. (15) was then used to model the net oxygen consumption flow $\dot{m}_{w,\mathrm{gen}O_2}$ (mg/h) in the fish tanks. Since all metabolite models are defined as a mass generation in the fish tanks, a minus sign in Eq. (15) must be present.

$$\dot{m}_{w,\mathrm{gen},O_2} = -60 r_{O_2} m_{w,\mathrm{BM}} \tag{15}$$

*2.1.2.3.3. Total ammonia nitrogen (TAN).* To calculate the TAN production rate, the same procedure was followed as for carbon dioxide. The calculated value used in the modelling was 0.289 mg/(kg min). Eq. (16) was used for calculating the TAN generation $\dot{m}_{w,\mathrm{gen},\mathrm{TAN}}$ (mg/h) in the fish tanks.

$$\dot{m}_{w,\mathrm{gen},\mathrm{TAN}} = 60 r_{\mathrm{TAN}} m_{w,\mathrm{BM}} \tag{16}$$

Where, $r_{\mathrm{TAN}}$ (mg/(kg min)) is the TAN production rate.

*2.1.2.3.4. Total suspended solids (TSS).* In contrast to other metabolites, TSS production was calculated in relationship to feed fed. All TSS was assumed to originate from feed and the TSS rate used in the model was expressed as such. Timmons and Ebeling (2010) specified a rule of thumb of 25 % of feed fed as TSS. In this study, the TSS fraction coming from feed $a_{\mathrm{TSS}}$ was 0.1605 $\mathrm{kg}_{\mathrm{TSS}}/\mathrm{kg}_{\mathrm{feed}}$. The TSS net mass flow production in the fish tanks $\dot{m}_{w,\mathrm{gen},\mathrm{TSS}}$ (mg/h) was calculated using Eq. (17).

$$\dot{m}_{w,\mathrm{gen},\mathrm{TSS}} = 10^6 a_{\mathrm{TSS}} \dot{m}_{w,\mathrm{Feed}} \tag{17}$$

Where, $\dot{m}_{w,\mathrm{Feed}}$ (kg/h) is the mass flow of feed added to the fish tanks.

### 2.1.3. Model parameters

A summary of all parameters used for validation of the simulated RAS is listed in Table 1. The parameters are for both the water treatment loop and the fish tank models.

## 2.2. Evaluating Matlab – Aspen HYSYS for RAS simulation

Modelling the recirculating water treatment loop in Aspen HYSYS is a viable method for RAS simulation. The built-in unit operations and equation packages greatly facilitate solving the processes with gas-liquid phase interaction such as the aerator and oxygen cones. Since the experimental efficiencies are used for model validation, calibrating the different unit operations is straightforward. The biofilter has the potential for including a more complex nitrification step and perhaps also including a denitrification step. In this work a flat conversion rate was found experimentally and implemented for all the simulations. However, the biofilter model can be extended in cases where enough experimental data from the biofilter is gathered to develop a more detailed nitrification model. Ways of performing this are: adding more chemical reactions that include other nitrogen species; developing an extended model for calculating the reaction conversion or, if the biofilter is dimensioned in detail and enough data is available, implementing a kinetic reaction set.

The simulation displays no stability nor convergence issues, but the simulated RAS operation has limited fluctuations, with no diurnal variations. Fish feeding and fish tank lighting is continuous and water temperature is regulated upon introduction of freshwater. The result is a RAS that operates mostly in a steady-state, except for the regulated oxygen cones bypass and for the case with adjusted recirculating water flow. The method and tools presented here, give satisfactory results for this quasi-dynamic simulation, but caution should be exercised when being implemented in dynamic systems with strong diurnal variations. Since the model and algorithm is validated for a very steady case, the robustness when simulating highly dynamic systems is still uncertain.

Simulations in which some variables experience steep rates of change, step functions are implemented with large changes, or where strong time dependencies are present, might encounter numerical instability. A poorly chosen time-step for the numerical integration could also be the cause of instabilities during the simulation. Divergence, occurrence of negative flows in the HYSYS simulation, or an unsolved water treatment loop could be a sign of a too large time-step. Typically, the time-step should be smaller than the hydraulic residence time of the fish tanks. Furthermore, adjustments to the time-step can be made according to the simulation's response. A small enough time-step will reduce the gradients on those parameters with very steep transient changes. However, too small a time-step will lead to unnecessary

**Table 1**
Validating parameters extracted from the experimental measurements and analysis, implemented in the RAS model in both Matlab and Aspen HYSYS.

| Parameter | Symbol | Value | Unit |
|---|---|---|---|
| Recirculating water flow | $Q$ | 24 | $m^3$/min |
| Fish tank overflow | $Q_{\mathrm{out}}$ | 80 | L/min |
| Specific growth rate | SGR | 1.93 | %/day |
| Feed ratio | %Feed | 1.54 | %/day |
| Drum filter efficiency | %TSS | 41.70 | %TSS removed |
| TAN conversion | %TAN | 45.26 | %TAN reacted |
| Overall $CO_2$ removal | $\%CO_2$ | 57.03 | $\%CO_2$ stripped |
| $O_2$ specific consumption rate | $r_{O_2}$ | 4.790 | mg/(kg min) |
| $CO_2$ specific production rate | $r_{CO_2}$ | 5.276 | mg/(kg min) |
| TAN specific production rate | $r_{\mathrm{TAN}}$ | 0.289 | mg/(kg min) |
| TSS production ratio | $a_{\mathrm{TSS}}$ | 0.1605 | $\mathrm{kg}_{\mathrm{TSS}}/\mathrm{kg}_{\mathrm{feed}}$ |

computational expense, and so a compromise between simulation speed and precision must be established, obtaining the maximum step-size which enables convergence to a specified degree of precision.

#### 2.2.1. Model limitations

- Fish tanks are treated as perfectly mixed tanks.
- Models used for mechanical filtration, carbon dioxide stripping, nitrification, and fish respiration and excretion were fitted using experimental data from the studied RAS. Their application to other cases might be limited and they would require refitting to appropriate data to extend their use to other RAS operational conditions and/or species.
- It is recommended to solve the HYSYS model prior to starting the iterative process. An unsolved HYSYS material stream could cause negative flows to appear on the next iteration. In this study, two built-in functions are incorporated: the first initializes and solves the HYSYS model and the second checks for correctly solved inlet water flows on every iteration.
- The hydraulic retention time between the fish tank outlet and inlet is assumed negligible since most of the system's volume is retained in the fish tanks. This means that the flow returning to the fish tanks is calculated for the same iteration (and time instant) as when the outlet water quality conditions are exported to Aspen HYSYS. For a system at steady state with no convergence problems like the one studied in this work, this does not suppose any setback. However, implementing the hydraulic retention time of smaller units should be considered for increasing precision in a system with sudden operational changes or with higher volumetric capacity on its water treatment units.

## 3. Results

The relative change of $CO_2$ concentrations in the fish tank outlet are displayed in Fig. 4. This figure shows a decreasing change which tends to zero in a time span of 8 simulated hours. All $CO_2$ concentrations converge as discussed in Section 2.1, since a uniform RAS operation throughout the day eliminates any possible daily variations in metabolite concentrations.

In all simulated weeks except the first week (week 2–15), the calculated relative change curves are clustered very tightly and no more than one curve could be distinguished. One single representative curve (orange) valid for weeks 2–15 is therefore plotted in Fig. 4. For week 1 (blue), the curve is farther from the cluster due to the unique initial conditions for the starting week of the grow-out. For further calculations, the converged value from each week was used as the representative operational conditions for that week.

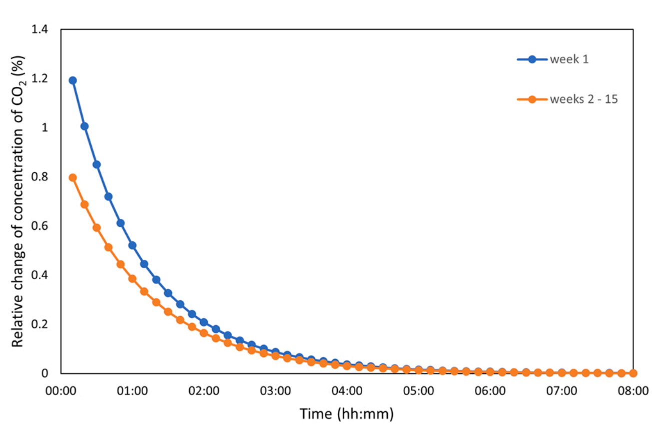


**Fig. 4.** Convergence of the simulation showing relative change of the concentration of $CO_2$. Curves for weeks 2–15 were clustered together and thus only one representative curve is shown.

### 3.1. Numerical stability analysis

To check the robustness of the model and tolerance to abrupt changes, stability studies were performed. In the first, a perturbation of four hours duration was introduced in the system to an already converged simulation on the eighth hour. The recirculating water flow, the freshwater flow, the fish tank overflows, the water flow through the oxygen cones and the blower air flow were all set to near-zero values. In a practical sense, this perturbation would recreate a complete stop in the recirculating water treatment loop, for example, due to a power outage. On the 12th hour, after the perturbation, all the pumps and the blower were switched on again to their normal operation and the recirculating water treatment loop started functioning again. The response of the water quality parameters is shown in Fig. 5a). During the second study, more frequent power outages were simulated in the same manner as the first case. Four cases were simulated where the duration of the perturbations was set to 30, 60, 90 and 120 min intervals. Each perturbation was followed by a normal RAS operation of equal duration. The cycle of perturbation and normal RAS operation was repeated 5 times for each case. The response of the water quality parameters for the case with 30 min perturbation intervals is shown in Fig. 5b) and Fig. 5c) shows the relative change of concentration at the end of the sequence of perturbations for all four cases.

Within eight hours after the perturbation, the metabolites' concentrations return to their original value, but at different rates. The DO level is the fastest to converge relative to the other metabolites due to the presence of the oxygen cones. After eight simulated hours, the relative change drops from 142 % to $2 \bullet 10^{-4}$ % as shown in Fig. 5a). For $CO_2$, TAN and TSS the convergence rate is slower since there are no components dedicated to regulating their concentrations. Instead, equilibrium is slowly approached as the water flows through the filter, biofilter and aerator on each water treatment loop pass. The relative change of $CO_2$, TAN and TSS are reduced from − 10 % to − 0.06 %, − 8 % to − 0.13 % and − 7 % to − 0.17 %, respectively.

TAN accumulates and is retained in the fish tanks during the system stop for four hours. Once the water starts flowing again, the higher TAN concentration reaches the biofilter and starts reacting into $NO_3$-N. Since $NO_3$-N is removed only with the fish tank overflows and system water exchange is estimated to be less than 7 % a slower convergence rate was expected. After eight hours, the relative change has been reduced to $-3.7 \bullet 10^{-3}$ % from a starting value of 0.11 % (Fig. 5a)).

When more frequent perturbations are introduced, no convergence is allowed to be reached due to the shorter time between changes in the recirculating water flow. Fig. 5b) shows how changes in the different metabolites reach a pattern of stable oscillation with each cycle. During each interval where recirculating water flow is shut down (e.g., between 08:00 and 08:30), DO decreases, and $CO_2$, TAN and TSS increase. $NO_3$-N remains constant since it is only generated once TAN is nitrified in the biofilter. Since water is not recirculating during this interval, TAN can only accumulate in the fish tanks. During the interval where flow is resumed (e.g., between 08:30 and 09:00), DO increases, and $CO_2$, TAN and TSS are reduced. The corresponding amount of reacted TAN in the biofilter is converted into $NO_3$-N, and hence $NO_3$-N increases. The trends during this interval follow a very similar pattern to the start of Fig. 5a).

Fig. 5c) shows that as perturbations last longer, water quality in the fish tanks worsen due to the recirculating treatment loop being offline. Despite the greater offset in water quality in the fish tanks, all metabolites return to their operational values during normal RAS operation. Longer intervals allow water quality to converge closer to the specified conditions. Comparing the cases for 30 and 120 min (Fig. 5c)), DO converges the fastest dropping from 2.79 % to 0.52 % relative change. The reductions in relative change go from − 5.60 % to − 3.81 % for $CO_2$, − 4.60 % to − 3.58 % for TAN, − 4.16 % to − 3.44 % for TSS, and 0.055 % to 0.032 % for $NO_3$-N.

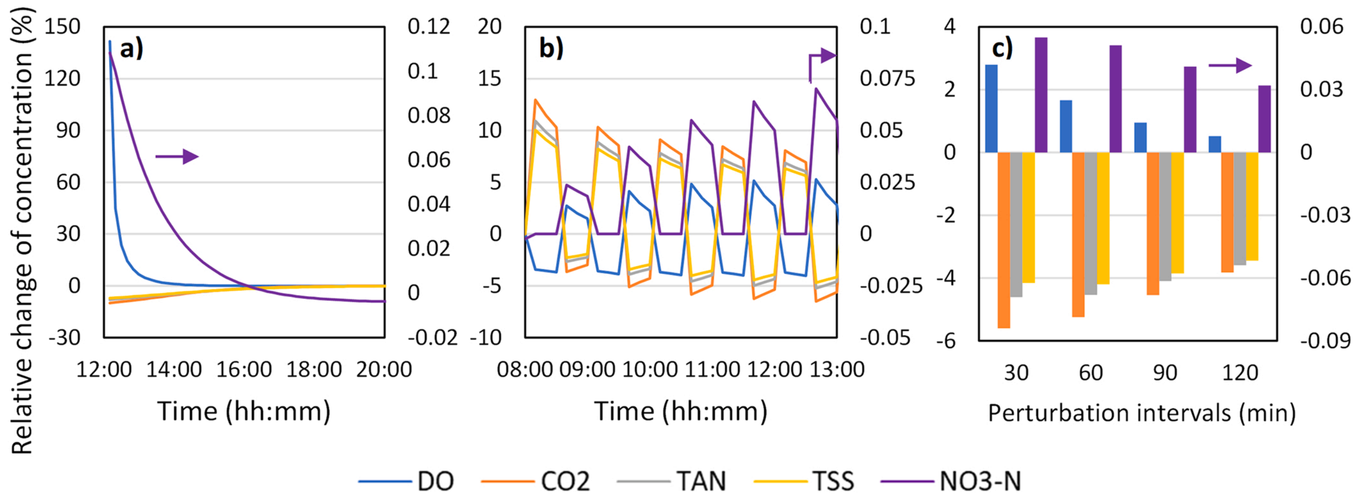


**Fig. 5.** Convergence of DO, $CO_2$, TAN, TSS (left axis) and $NO_3$-N (right axis) concentrations in the fish tanks after a perturbation in the RAS operation. Convergence is shown **a)** after a single perturbation of 4 h, **b)** for consecutive perturbations of 30 min, and **c)** at the end of different perturbation intervals.

### 3.2. Metabolite concentrations

Weekly concentration values after convergence of all investigated metabolites in the fish tanks are shown in Fig. 6. DO keeps a very stable trend at 9.5 mg/L except for the first two weeks where the values are slightly higher. Carbon dioxide is kept within advisable limits for most of the simulation time but surpasses the 10 mg/L mark by week 12. By the end of the simulation at week 15 a peak of 16.06 mg/L is reached. The amount of TAN in the fish tanks is kept within safe levels during the full stocking period. The highest estimated TAN concentration and the only one crossing the 1 mg/L threshold is 1.05 mg/L on the last week. The highest TSS concentration value found in the simulation is 6.79 mg/L by the end of the grow-out when daily feed masses are greatest. In this simulation the $NO_3$-N concentration starts at 18.08 mg/L. By the end of the grow-out period, it goes as high as 119.7 mg/L $NO_3$-N.

### 3.3. RAS energy demand with constant recirculating water flow

The energy demand and the fraction of energy demand of all equipment in the RAS model is gathered in Fig. 7a) and Fig. 8a), respectively.

Fish tank lighting has the most marginal demand of all considered equipment, even though lighting was on 24 h a day. The unchanged lighting program throughout the grow-out is reflected on its demand, which remains constant at 76.8 kWh/day. This represents a demand between 1.10 % and 1.56 % of the total energy demand during the 15 simulated weeks as seen in Fig. 8a). Similarly, the blower also shows a flat energy demand on all weeks. At 1.466 MWh/day, its energy demand with respect to the total is between 21.1 % and 29.7 %.

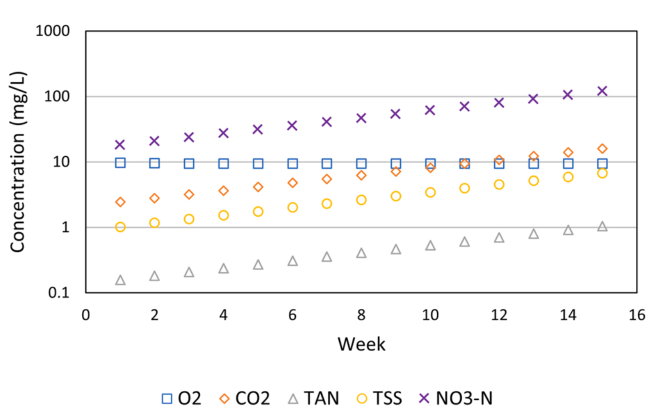


**Fig. 6.** Water quality parameters in the simulated fish tanks for each week of the full grow-out period with constant recirculating water flow.

Input freshwater requires the greatest amount of thermal energy for the majority of the grow-out. It is only surpassed by the centrifugal pump to the oxygen cones during weeks 13–15. The thermal energy requirement starts at 1.891 MWh/day and steadily ramps up to 1.923 MWh/day by the last week. That is 38.3 % and 27.7 % of total energy demand for the starting and ending week, respectively. The reason energy demand was not constant is the slight increase of required freshwater to compensate for water exchange and system losses. As more feed is needed to satiate growing fish, more water is lost with removed TSS in the drum filters. These results are arguably overestimated, and the energy demand is actually a fraction of the reported from the simulation. In the RAS facility, fish tank overflows are sent to heat exchangers to pre-heat the freshwater. Then, a heat pump warms the preheated freshwater up to the systems temperature. In contrast, results from this simulation only show the thermal energy demand to raise the freshwater temperature from 5 °C to 12 °C, which are the freshwater's and system's temperatures respectively.

The RAS recirculating water pumps show a wider range of energy demand. When all recirculating water is pumped through these pumps, demand is at its highest at 1.498 MWh/day or 30.4 % of total energy demand. However, it starts dropping once more water is drawn by the pump to the oxygenators and less water needs to be pumped through the main RAS pumps. By week 15, water volume pumped by RAS recirculating pumps is at its lowest, demanding 1.293 MWh/day or 18.6 % of total energy demand.

The pump to the bypass where the oxygen cones are installed, shows the most dramatic change in energy demand throughout the simulation. For weeks 1 and 2, the bypass is closed due to DO levels being high enough for the low biomass of the fish tanks. This contrasts with Fig. 6 where DO in the fish tanks is above its set point of 9.5 mg/L. As fish grow and more oxygen is needed, more water is pumped into the oxygen cones and the energy demand of the pump rises accordingly. For weeks 13–15, the oxygen cones pump becomes the largest consumer. By the end of the grow-out, the energy demand is 2.196 MWh/day or 31.6 % of total energy demand.

In absolute terms, the RAS model needs a total energy of 4.933 MWh/day in the beginning, which stays constant until the pump to the oxygen cones is turned on. Then it follows a very similar trend as the oxygen cones pump until total energy demand ends on a maximum of 6.955 MWh/day. The energy necessary for operating the RAS from start to end of the grow-out is 663.8 MWh.

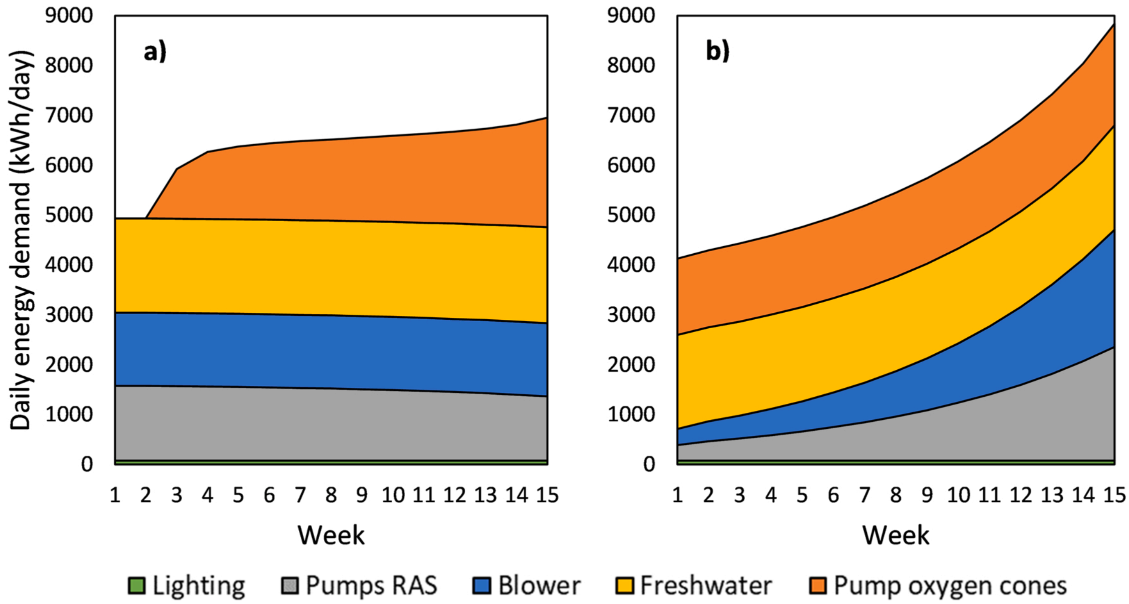


**Fig. 7.** Energy demand of all simulated RAS equipment for the full grow-out period with **a)** constant, and **b)** adjusted recirculating water flow.

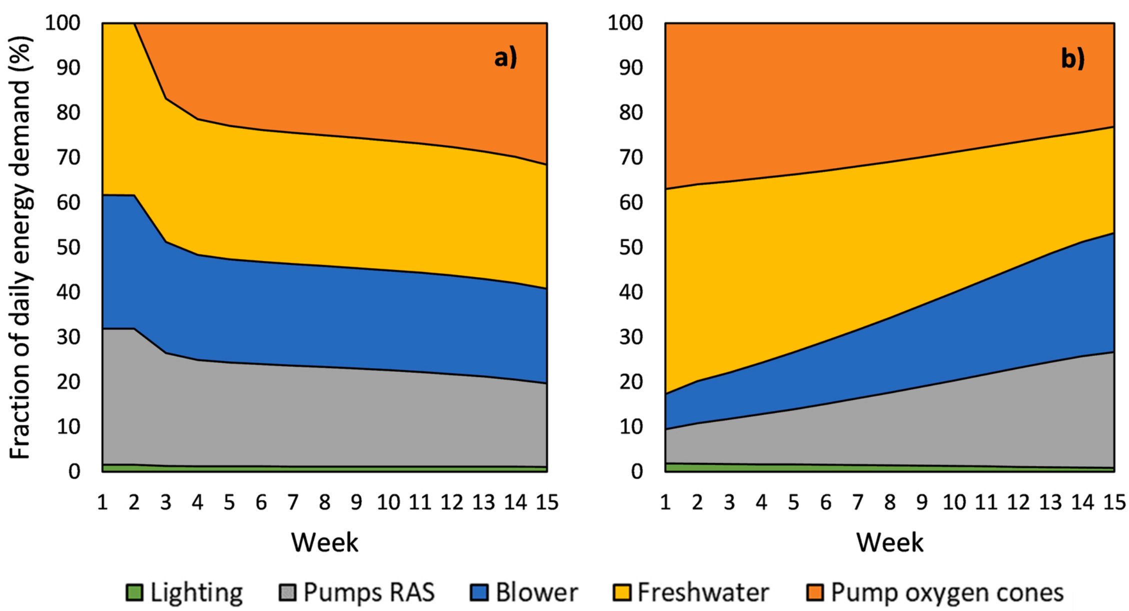


**Fig. 8.** Fraction of the daily energy demand of all simulated RAS equipment for the full grow-out period with **a)** constant, and **b)** adjusted recirculating water flow.

The results on specific energy demand for all simulated energy demanding equipment and RAS as a whole are listed in Table 2. The specific energy demand of the simulated RAS is 9.586 kWh/kg. Almost one third of the energy is dedicated to covering the freshwater thermal energy requirements. In reality, the magnitude would be lower since what is reported here is the difference of thermal energy of freshwater between 5 °C and 12 °C.

**Table 2**
Energy demand of RAS equipment for the simulations with constant and adjusted recirculating water flow.

| | Fraction of total energy demand (%) | | Specific energy demand (kWh/kg) | | Difference (%) |
|---|---|---|---|---|---|
| Operation schedule | Constant | Adjusted | Constant | Adjusted | |
| Blower | 23.19 | 18.37 | 2.223 | 1.622 | - 27.06 |
| Pump oxygen cones | 22.90 | 29.50 | 2.196 | 2.604 | 18.56 |
| Pumps RAS | 22.58 | 17.90 | 2.163 | 1.580 | - 26.96 |
| Freshwater | 30.10 | 32.91 | 2.887 | 2.905 | 0.624 |
| Lighting | 1.21 | 1.32 | 0.117 | 0.117 | 0 |
| Total | | | 9.589 | 8.827 | - 7.92 |

Recirculating pumps account for 22.6 % of the total energy demand for the whole period. Including the pump to the oxygen cones, all pumps are responsible for 45.48 % of all energy demand. This is 4.359 kWh/kg in specific energy terms. There is a possibility to reduce energy demand of RAS pumps by regulating down the flow when possible. This applies mostly to the weeks when the RAS is operating well below its design conditions.

### 3.4. RAS energy demand with adjusted recirculating water flow

An alternative operation schedule to reduce overall energy demand is investigated. The recirculating water pumps of the main water treatment loop are adjusted to pump the minimum necessary water to keep water quality parameters in the fish tanks within acceptable levels. The allowable upper limits are 10 mg/L for carbon dioxide, 1 mg/L for TAN and 80 mg/L for TSS. DO in the fish tanks is regulated at 9.5 mg/L using the oxygen cones bypass in the same manner as with constant recirculating water flow. In this operation mode, all water parameters will be within the established limits except for one (the bottleneck parameter), which will remain at the boundary.

Air sent through the blower and into the aerator needs to be adjusted accordingly, too. Since the total carbon dioxide stripping efficiency per pass must match the experimental measurements, the air-to-water ratio needs to be regulated.

Water quality parameters for the simulation with adjusted recirculating water flow are as follows: Carbon dioxide in the fish tanks is very close or equal to 10 mg/L in all weeks. It can be established that carbon dioxide is the system's bottleneck parameter. DO is at 9.5 mg/L in the fish tanks except for the first 4 weeks where it hovers slightly above this value. The highest DO is found in week 1 at 9.72 mg/L which is not much higher than the desired value. TAN concentrations remain stable throughout the simulation ranging between 0.529 and 0.641 mg/L.

The recirculating water flow starts at 5.50 $m^3$/min and steadily increases until it reaches a maximum flow of 39.41 $m^3$/min by the final week. Water flow is 26.26 $m^3$/min by week 12, which surpasses the value for the case with constant water flow (24 $m^3$/min). This is justified since the carbon dioxide concentration crosses the 10 mg/L limit on week 12 when water flow is constant, as shown in Fig. 6. Thus, the need for a larger flow to keep the $CO_2$ level within its limit in the adjusted flow case arises.

The energy demand results for the adjusted water flow case are shown in Fig. 7b) and Fig. 8b). The blower and the recirculating RAS pumps are responsible for a large variation in the RAS total energy demand as weeks pass and the culture is intensified. The energy demand for the blower and RAS pumps is only 325 and 313 kWh/day at the beginning, with ending values of 2.343 and 2.283 MWh/day, respectively. The oxygen cones pump also shows an increasing but flatter trend with a starting and ending energy demand of 1.526 and 2.040 MWh/day, respectively. The thermal energy requirements of entering freshwater keep a narrow and stable trend that starts at 1.885 MWh/day and reaches 2.099 MWh/day by the final week. Lighting energy demand is unaffected by the change in RAS operation mode and remains at 76.8 kWh/day. The RAS total energy demand shows an upward trend during the grow-out, starting at 4.127 MWh/day and ending at 8.842 MWh/day, needing a total aggregated energy demand of 611.1 MWh for the whole operation.

The specific energy demand adjusting the recirculating water flow is 8.827 kWh/kg (see Table 2). The freshwater thermal energy requirements are the largest at 2.905 kWh/kg followed closely by the oxygen cones pump at 2.604 kWh/kg. The blower and the RAS pumps show a very similar energy demand at 1.622 and 1.580 kWh/kg, respectively.

In relative terms, the blower and the RAS pump demand 27.06 % and 26.96 % less energy when water flow is adjusted, respectively. In contrast, the oxygen cones pump shows an increase of 18.56 % for the case with adjusted flow. This larger energy demand is caused by the main recirculating flow being reduced most weeks compared to the case with constant flow. Since the net mass flow of oxygen sent to the fish tanks from the aerator is smaller, more water needs to be sent to the oxygen cones to satisfy the desired DO level in the fish tanks. The thermal requirement of freshwater is marginally increased by 0.624 % when water flow is adjusted, and fish tanks lighting has an identical energy demand for both cases. Overall, the energy demand of the RAS is 7.92 % less when the recirculating water flow of the main treatment loop is adjusted accordingly to water quality in the fish tanks.

## 4. Discussion

The water quality and model validation parameters for the fish tanks are compared to literature and scrutinized in this section. RAS energy demand and the effect of adjusting the water recirculating water flow on energy demand and water quality is discussed in detail.

### 4.1. Specific growth rate (SGR)

The similarity of literature values with the implemented growth of 1.93 % was difficult to evaluate due to a broad variability of operational conditions. The cases with most similar conditions were chosen for comparison and the specific growth rate was found to be 1.10–1.85 % for Atlantic salmon with a BW of 10–700 g (Fivelstad et al., 2007; Handeland et al., 2008; Imsland et al., 2014; Shi et al., 2016; Sun et al., 2016). In all instances, the reported SGR values were below the SGR measured and used in this study. This could be explained by the RAS continuous operation mode with a 24-h constant lighting and feeding.

### 4.2. Carbon dioxide ($CO_2$)

There is a notorious difference between the carbon dioxide production rate in the literature and the rate used in this study's RAS model, which was taken from experimental measurements. The carbon dioxide production rate of Atlantic salmon in the same BW range (60–150 g) was measured at 2.1–2.2 mg/(kg min) (Kvamme et al., 2019). A similar rate of 2.13 mg/(kg min) was obtained for adult fish of 2 kg BW with continuous feeding and a feed ratio of 0.59 % (Forsberg, 1997). This difference can be noticed when operating or simulating the RAS in the form of unexpectedly high $CO_2$ concentrations in the fish tank outlet. It is possible that the assumed carbon dioxide production when the system was designed might have been lower than the actual one. In any case, carbon dioxide concentration in the fish tanks surpasses the 10 mg/L limit recommended for Atlantic salmon (Lawson, 1995; Thorarensen and Farrell, 2011) after week 12. A slightly higher limit of 10.6 mg/L can also be considered safe (Fivelstad et al., 1998). At the end of the simulation carbon dioxide concentration peaks at 16.06 mg/L. The advised upper concentration limits has been established by investigating a set of fish health indicators, SGR among them. Too high $CO_2$ levels in the fish tanks could risk compromising fish welfare as well as underperformance of the RAS. There are two possible explanations for this unexpected rise in $CO_2$. One is that the carbon dioxide stripping capacity of the RAS might be limited. The returning water flow to the fish tanks still has potential for further carbon dioxide removal. The other more plausible explanation is an unexpectedly high carbon dioxide production rate. Comparing the experimental carbon dioxide production rate in Section 2.1.2.3.1 with literature, a suspiciously wide discrepancy appears. The experimental value is at least twice as large as expected. Considering a carbon dioxide production rate on the same range as on the literature, the full grow-out stage could have been completed without $CO_2$ exceeding its recommended limit. To verify this, a sensitivity analysis was performed where the carbon dioxide production rate in the fish tanks $r_{CO_2}$ was specified as 50 % of the original rate. The simulation with a constant recirculating water flow of 24 $m^3$/min was performed in the same manner, and the new carbon dioxide concentrations were observed in the fish tanks. At the start of the grow out, the concentration is 1.22 mg/L, and it increases until the peak concentration of 8.05 mg/L is reached by week 15. The water quality is always kept within the recommended limit which indicates that an excessively large carbon dioxide production rate could be the reason the limit was surpassed on the original simulation.

### 4.3. Oxygen (DO)

The choice of keeping the DO level at 9.5 mg/L in the fish tanks is both supported by operational practices from the original RAS this work is based on, as well as literature. A high DO level that does not surpass 100 % saturation is the recommendation for Atlantic salmon according to the Norwegian Veterinary Institute (Fiskehelserapporten, 2022). Other findings agree with this guideline. A DO between 5 mg/L and full saturation is recommended in Lawson (1995) and a narrower range of 80–100% saturation is suggested in Thorarensen and Farrell (2011). The two first simulated weeks in the case with constant recirculating water flow the DO is above 9.5 mg/L. The explanation for this is the low fish biomass in the fish tanks. This leads to a lower oxygen respiration than the system is designed for. As a result, oxygen cones are not used during the first two weeks because enough oxygen is already being introduced to the water flow in the biofilter and aerator. Thus, a resultant higher DO level than the target value set for the fish tanks. The trend stabilizes at week 3, where a higher oxygen consumption rate forces the use of the oxygen cones to regulate the DO in the fish tanks at 9.5 mg/L.

Oxygen consumption rates range between 1.10 and 12.0 mg/(kg min) with BW varying correspondingly between 1 g and 2000 g (Bergheim et al., 1991; Fivelstad et al., 1999; Fivelstad and Smith, 1991; Forsberg, 1997; Forsberg and Bergheim, 1996; Grøttum and Sigholt, 1998; Wiggs et al., 1989).

### 4.4. Total ammonia nitrogen (TAN)

The same pattern as with carbon dioxide and oxygen can be observed when comparing the TAN production rate with the literature. The highest reported TAN production rate is still below the implemented experimental value. The TAN production rate in the literature varies between 0.056 mg/(kg min) and 0.23 mg/(kg min) (Bergheim et al., 1991; Fivelstad et al., 1990; Forsberg, 1997; Kvamme et al., 2019; Wiggs et al., 1989).

A recommended upper TAN concentration limit for Atlantic salmon is 1 mg/L (Lawson, 1995). In this case, week 15 is the only instance when TAN crosses the limit. However, a study on effects of TAN in Atlantic salmon reported a mean value of 1.26 mg/L to be safe (Fivelstad et al., 1995). It is a subjective matter to conclude whether TAN levels were completely within acceptable limits, depending on which source is to be strictly followed. In any case, the exposure to a concentration slightly higher than 1 mg/L lasted only for one week.

### 4.5. Total suspended solids (TSS)

With a maximum recommended TSS concentration of 80 mg/L (Lawson, 1995) and a maximum simulated value of 6.75 mg/L, TSS is the parameter with least concern for reaching its set limit.

### 4.6. Nitrate nitrogen ($NO_3$-N)

The concentration of $NO_3$-N increases steadily throughout the grow out and peaks at a concentration of 119.7 mg/L by week 15. In the literature, Lawson (1995) gives a recommendation of keeping the $NO_3$-N concentration lower than 3 mg/L. However, this threshold falls short compared to recent findings. In one study, Atlantic salmon growth was suggested to be relatively unaffected by $NO_3$-N concentrations up to 101.8 mg/L (Freitag et al., 2015). Another study concludes that 100 mg/L $NO_3$-N is a safe level for Atlantic salmon culture (Davidson et al., 2017).

Since there is no removal of $NO_3$-N in the system (e.g., presence of a denitrification step), $NO_3$-N can only be removed through the fish tank overflows. The large accumulation of $NO_3$-N could then be caused by too low of a daily water exchange which is estimated to be less than 7 % in the modelled RAS case. Unfortunately, there is little research on the effect of higher $NO_3$-N concentrations on Atlantic salmon. As Davidson et al. (2017) proposed, additional research beyond the 100 mg/L $NO_3$-N mark is needed. Regarding the live culture, growth was not impaired, but no study assessing health indicators was performed. It would be advisable to increase the overflows and water exchange of the system or incorporate a denitrification filter with intent to reduce $NO_3$-N concentrations to 100 mg/L when at maximum capacity. A reevaluation of this measure can be done once there is broader knowledge on the effects of higher $NO_3$-N concentrations on Atlantic salmon.

### 4.7. Energy demand with adjusted water flow

From an energy perspective, adjusting the water flow of the RAS is a viable option to reduce demand. RAS energy demand was reduced by 7.92 % when water flow was adjusted following simple criteria, but a more efficient water flow control may exist. The energy demand of the oxygen cones pump should also be considered when finding the operational conditions with minimized energy demand. A reduction in the main recirculating water flow can cause more water to be pumped through the oxygen cones to compensate for the diminished net oxygen mass flow introduced in the aerator. Additionally, the pump to the oxygen cones might need to be turned on when the water flow is adjusted on weeks where it normally would not be if the water flow was a constant 24 $m^3$/min, such as the first two weeks of the simulated scenarios. A trade-off between the main water treatment loop and the oxygen cones secondary loop should be established. The optimum water flows to be adjusted should be found based on the combined energy demand of the blower, RAS pumps and oxygen cones pump.

Adjusting the water flow directly affects the water quality in the fish tanks. When recirculating water is reduced, the water quality diminishes. Since water quality is being leveraged to reduce energy demand, it is crucial to keep a level of water quality that does not impair fish welfare. In this study, carbon dioxide is the bottleneck parameter for regulating the recirculating water flow. The maximum allowable carbon dioxide concentration in the fish tanks is set at 10 mg/L which, according to literature, has no harmful effects after long term exposure.

When comparing the case with adjusted water flow against the case with constant one, the relationship between recirculating water flow and carbon dioxide concentration becomes clear. From weeks 1 to 11, $CO_2$ in the fish tanks is below the 10 mg/L limit when water flow is constant. The difference between $CO_2$ and the set threshold is traded off for a lower recirculating water flow when flow adjustment is allowed. An opposite trend happens between weeks 12 and 15. Since the concentration of carbon dioxide surpasses the threshold in the constant water flow case, a water flow increase must be implemented to reduce the concentration to the set limit. The last four simulated weeks are, in fact, more energy demanding when water flow is adjusted because water quality in the base case was not complying with the defined water quality standards. Nevertheless, a reduction of 7.92 % energy demand is still possible when water flow is adjusted during the grow-out period while simultaneously keeping all water quality parameters within their set limits for fish welfare.

The RAS energy demand can be further reduced if the set limits for the water quality parameters in the fish tanks are less strict. However, the water quality parameters should not be allowed to worsen beyond fish comfort levels in benefit of increased energy savings. A note of caution needs to be made to prevent possible non-fish friendly practices to be justified from this work. At no point is fish welfare sacrificed for a lower RAS energy demand. To be precise, water quality in the simulated fish tanks was allowed to slightly worsen within acceptable limits as to not cause any negative effects on fish welfare. Any further investigation for the reduction of RAS energy demand should first comply with a water quality standard for fish welfare.

## 5. Conclusion

This paper demonstrates the viability of Aspen HYSYS for recirculating aquaculture systems modelling and simulation automated from Matlab. To the knowledge of the authors, this is the first time a RAS or part of it (i.e., the recirculating water treatment loop) is modelled and validated in Aspen HYSYS. The model also serves to replicate the operating conditions of a case study RAS.

A numerical stability analysis was performed on the RAS model to test its viability when simulating a stop in one or several units central to the recirculating water treatment loop such as pumps or blowers. The results indicate that abrupt changes do not lead to divergence and the simulation is able to converge once the normal operation is resumed.

Concentrations of $CO_2$, DO, TSS, TAN and $NO_3$-N in the fish tanks were produced based on weekly operation conditions. Energy demand of equipment central to the RAS operation was calculated for a single full grow-out period.

One concerning result is that the $CO_2$ concentration in the fish tanks surpasses the recommended threshold after week 12. The most reasonable explanation is the excessively high $CO_2$ production rate of 5.276 mg/(kg min) which more than doubles reported literature values. In a sensitivity analysis where the RAS was simulated with a carbon dioxide production rate of 2.638 mg/(kg min) the $CO_2$ concentration never exceeded the recommended limit. The unexpectedly high carbon dioxide production rate is arguably the reason water quality was not met by the end in terms of $CO_2$ concentration. The cause for this high $CO_2$ production rate should therefore be investigated further. Alternatively, improving the carbon dioxide stripping efficiency of the system would allow the RAS to stock a larger biomass. Or, in the case of a set growth schedule, this would facilitate keeping lower levels of $CO_2$.

The accumulated $NO_3$-N in the system is caused by the absence of a denitrification step in the biofilter and by low water exchange. However, no clear answer to the effects of $NO_3$-N concentrations above 100 mg/L can be offered due to lacking literature.

Levels of DO, TAN and TSS are all within acceptable limits. DO is regulated throughout the whole operation and kept at 9.5 mg/L in the fish tanks. TAN concentration comes close to its recommended limit by the end of the grow-out. TSS in the fish tanks is not only well controlled, but the concentration at largest biomass is less than ten times below the recommended upper limit.

The specific energetic cost of growing Atlantic salmon post-smolts is 9.589 kWh/kg. In total, RAS energy demand for the whole grow-out operation is 663.8 MWh. 45.48 % of this total is needed to operate all system pumps (i.e., both RAS pumps and the oxygen cones pump). After pumps, freshwater thermal energy requirements account for 30.10 % of total energy demand. The energy need for the air blower constitutes 23.19 % of the overall energy need and a marginal 1.21 % is dedicated to fish tank lighting.

In an alternative proposed operation, recirculating water flow is adjusted to reduce energy demand. The blower and recirculating pumps energy demand are approximately 27 % less than with constant water recirculating flow, whilst the energy demand of the pump to the oxygen cones increases by 18.56 %. In overall terms, the RAS energy demand is reduced by 7.92 % when recirculating water flow is adjusted with a specific energy demand of 8.827 kWh/kg. This suggests alternative, more efficient operation is possible and future work will consider optimised RAS operation within a wider system of a grid-independent, renewably sourced energy system.

## Data Availability/Conflicts of interest

Data used for the modelling and validation of the RAS was obtained from two different parties. Details on installed equipment were provided by Kari Attramadal and Geir Løvik (Nofitech). These include pump and compressor models, technical diagrams for correctly building the sequence of the water treatment loop and design parameters such as recirculated and oxygenated water flows, pressures, and temperatures. Operational data was measured at ERKO Settefisk (Stord, Norway), which included water flows and analyses for various water quality parameters at different locations of the RAS.

## CRediT authorship contribution statement

**Gerard Ayuso VIrgili:** Conceptualization, Methodology, Software, Validation, Resources, Data curation, Writing – original draft, Writing – review & editing, Visualization. Leila Jafari: Investigation, Resources, Writing – review & editing. **David Lande-Sudall:** Conceptualization, Methodology, Writing – review & editing, Supervision. **Norbert Lümmen**: Conceptualization, Methodology, Writing – review & editing, Supervision.

## Declaration of Competing Interest

The authors declare that they have no known competing financial interests or personal relationships that could have appeared to influence the work reported in this paper.

## Data Availability

The data that has been used is confidential.

## Acknowledgements

This research was financially supported by The Research Council of Norway (Project no. 301828) and Western Norway University of Applied Sciences. The authors thank Kari Attramadal and Geir Løvik (Nofitech) for offering the necessary data for modelling the RAS and answering questions critical to the correct RAS design in HYSYS, Kjell Eivind Frøysa (Western Norway University of Applied Sciences) for helpful discussions, Rune Sandvik (ERKO Settefisk) for access to the RAS facility, and bachelor students Ida Pettersen and Tommy Engevik for assisting with water sampling, analysis, and flow measurements at ERKO Settefisk.

## References

Badiola, M., Basurko, O.C., Gabiña, G., Mendiola, D., 2017. Integration of energy audits in the Life Cycle Assessment methodology to improve the environmental performance assessment of recirculating. Aquac. Syst. J. Clean. Prod. 157, 155–166.
Badiola, M., Basurko, O.C., Piedrahita, R., Hundley, P., Mendiola, D., 2018. Energy use in Recirculating Aquaculture Systems (RAS): a review. Aquac. Eng. 81, 57–70.
Bergheim, A., Nilsen, A., 2015. Intensification of Salmonid Aquaculture. Athens ATINER'S Conf. Pap. Ser. No WAT2015-1652.
Bergheim, A., Seymour, E.A., Sanni, S., Tyvold, T., Fivelstad, S., 1991. Measurements of oxygen consumption and ammonia excretion of Atlantic salmon (Salmo salar L.) in commercial-scale, single-pass freshwater and seawater landbased culture systems. Aquac. Eng. 10, 251–267.
d'Orbcastel, E.R., Blancheton, J.P., Aubin, J., 2009. Towards environmentally sustainable aquaculture: comparison between two trout farming systems using Life Cycle Assessment. Aquac. Eng. 40, 113–119.
Dalsgaard, J., Lund, I., Thorarinsdottir, R., Drengstig, A., Arvonen, K., Pedersen, P.B., 2013. Farming different species in RAS in Nordic countries: current status and future perspectives. Aquac. Eng. 53, 2–13.
Davidson, J., Good, C., Williams, C., Summerfelt, S.T., 2017. Evaluating the chronic effects of nitrate on the health and performance of post-smolt Atlantic salmon Salmo salar in freshwater recirculation aquaculture systems. Aquac. Eng. 79, 1–8.
Ernst, D.H., Bolte, J.P., Nath, S.S., 2000. AquaFarm: simulation and decision support for aquaculture facility design and management planning. Aquac. Eng. 23, 121–179.
FAO, 2022. Food and Agriculture Organization of the United Nations. Int. Organ. vol. 1, pp. 350–3.
Fiskehelserapporten, 2022. Rapport 2a/2022 Veterinærinstitutet - Norwegian Veterinary Institute.
Fiskeridirektoratet, 2020a. Statistikk for akvakultur 2009 46.
Fiskeridirektoratet, 2020b. Statistikk for akvakultur 2019 46.
Fivelstad, S., Smith, M.J., 1991. The oxygen consumption rate of Atlantic salmon (Salmo salar L.) reared in a single pass landbased seawater system. Aquac. Eng. 10, 227–235.
Fivelstad, S., Thomassen, J.M., Smith, M.J., Kjartansson, H., Anne-Britt, Sandø, 1990. Metablite production rates from Atlantic salmon (Salmo salar L.) and Arctic char (Salvelinus alpinus L.) reared in single pass land-based brackish water and sea-water systems. Aquac. Eng. 9, 1–21.
Fivelstad, S., Schwarz, J., Strømsnes, H., Olsen, A.B., 1995. Sublethal effects and safe levels of ammonia in seawater for Atlantic salmon postsmolts (Salmo salar L.). Aquac. Eng. 14, 271–280.

Fivelstad, S., Haavik, H., Løvik, G., Olsen, A.B., 1998. Sublethal effects and safe levels of carbon dioxide in seawater for Atlantic salmon postsmolts (Salmo salar L.): ion regulation and growth. Aquaculture 160, 305–316.
Fivelstad, S., Bergheim, A., Kløften, H., Haugen, R., Lohne, T., Berit Olsen, A., 1999. Water flow requirements in the intensive production of Atlantic salmon (Salmo salar L.) fry: growth and oxygen consumption. Aquac. Eng. 20, 1–15.
Fivelstad, S., Waagbø, R., Stefansson, S., Olsen, A.B., 2007. Impacts of elevated water carbon dioxide partial pressure at two temperatures on Atlantic salmon (Salmo salar L.) parr growth and haematology. Aquaculture 269, 241–249.
Forsberg, O.I., 1997. The impact of varying feeding regimes on oxygen consumption and excretion of carbon dioxide and nitrogen in post-smolt Atlantic Salmon Salmo salar L. Aquac. Res. 28, 29–41.
Forsberg, O.I., Bergheim, A., 1996. The impact of constant and fluctuating oxygen concentrations and two water consumption rates on post-smolt atlantic salmon production parameters. Aquac. Eng. 15, 327–347.
Freitag, A.R., Thayer, L.A.R., Leonetti, C., Stapleton, H.M., Hamlin, H.J., 2015. Effects of elevated nitrate on endocrine function in Atlantic salmon, Salmo salar. Aquaculture 436, 8–12.
Grøttum, J.A., Sigholt, T., 1998. A model for oxygen consumption of Atlantic salmon (Salmo salar) based on measurements of individual fish in a tunnel respirometer. Aquac. Eng. 17, 241–251.
Handeland, S.O., Imsland, A.K., Stefansson, S.O., 2008. The effect of temperature and fish size on growth, feed intake, food conversion efficiency and stomach evacuation rate of Atlantic salmon post-smolts. Aquaculture 283, 36–42.
Hilmarsen, Ø., Ambros Holte, E., Brendeløkken, H., Høyli, R., Hognes, E.S., 2018. Konsekvensanalyse av landbasert oppdrett av laks – matfisk og post-smolt.
Imsland, A.K., Handeland, S.O., Stefansson, S.O., 2014. Photoperiod and temperature effects on growth and maturation of pre- and post-smolt Atlantic salmon. Aquac. Int. 22, 1331–1345.
Kamali, S., Ward, V.C.A., Ricardez-Sandoval, L., 2022. Dynamic modeling of recirculating aquaculture systems: effect of management strategies and water quality parameters on fish performance. Aquac. Eng. 99, 102294.
Karimanzira, D., Keesman, K.J., Kloas, W., Baganz, D., Rauschenbach, T., 2016. Dynamic modeling of the INAPRO aquaponic system. Aquac. Eng. 75, 29–45.
Kvamme, K., Fivelstad, S., Handeland, S.O., Bergheim, A., 2019. Water flow and diurnal variation in metabolite production rates of Atlantic salmon ( Salmo salar L.) post-smolt. Aquac. Res. 50, 323–330.
Lawson, T.B., 1995. Fundamentals of Aquacultural Engineering [WWW Document]. 〈https://books.google.no/books?hl=no&lr=&id=cXF8gzWFWEYC&oi=fnd&pg=PP9&ots=RblSDHjYx7&sig=VqzV0x6BVHXf9AH-_4_o7AKATH0&redir_esc=y#v=onepage&q&f=false〉, (Accessed 5 April 2022).
Rusten, B., Eikebrokk, B., Ulgenes, Y., Lygren, E., 2006. Design and operations of the Kaldnes moving bed biofilm reactors. Aquac. Eng. 34, 322–331.
Samuel-Fitwi, B., Nagel, F., Meyer, S., Schroeder, J.P., Schulz, C., 2013. Comparative life cycle assessment (LCA) of raising rainbow trout (Oncorhynchus mykiss) in different production systems. Aquac. Eng. 54, 85–92.
Sanni, S., Forsberg, O.I., 1996. Modelling pH and carbon dioxide in single-pass sea-water aquaculture systems. Aquac. Eng. 15, 91–110.
Shi, C., Liu, Y., Yi, M., Zheng, J., Tian, H., Du, Y., Li, X., Sun, G., 2016. Comparison of time-restricted and ad libitum self-feeding on the growth, feeding behavior and daily digestive enzyme profiles of Atlantic salmon. Chin. J. Oceanol. Limnol. 729–736, 2017 354 35.
Sun, G., Liu, Y., Qiu, D., Yi, M., Li, X., Li, Y., 2016. Effects of feeding rate and frequency on growth performance, digestion and nutrients balances of Atlantic salmon (Salmo salar) in recirculating aquaculture systems (RAS). Aquac. Res. 47, 176–188.
Tanveer, M., Moulick, S., Mukherjee, C.K., 2020. Mathematical model for goldfish recirculating aquaculture system (GRAS). Aquac. Eng. 90, 102092.
Thorarensen, H., Farrell, A.P., 2011. The biological requirements for post-smolt Atlantic salmon in closed-containment systems. Aquaculture 312, 1–14.
M.B. Timmons J.M. Ebeling Recirculating Aquaculture 2nd Edition 2010.
Varga, M., Csukas, B., Kucska, B., 2020. Implementation of an easily reconfigurable dynamic simulator for recirculating aquaculture systems. Aquac. Eng. 90.
Wiggs, A.J., Henderson, E.B., Saunders, R.L., Kutty, M.N., 1989. Activity, respiration, and excretion of ammonia by Atlantic salmon ( Salmo salar) smolt and postsmolt. Can. J. Fish. Aquat. Sci. 46, 790–795.
Wik, T.E.I., Lindén, B.T., Wramner, P.I., 2009. Integrated dynamic aquaculture and wastewater treatment modelling for recirculating aquaculture systems. Aquaculture 287, 361–370.
Yogev, U., Gross, A., 2019. Reducing environmental impact of recirculating aquaculture systems by introducing a novel microaerophilic assimilation reactor: modeling and proof of concept. J. Clean. Prod. 226, 1042–1050.
Yogev, U., Sowers, K.R., Mozes, N., Gross, A., 2017. Nitrogen and carbon balance in a novel near-zero water exchange saline recirculating aquaculture system. Aquaculture 467, 118–126.

**Gerard Ayuso Virgili** is a Ph.D. candidate in the Ph.D. Programme in Computer Science at the Western Norway University of Applied Sciences. He has a master's degree in Chemical and Process Engineering from University of Rovira i Virgili/ Norwegian University of Science and Technology. His research is focused on energy demand in recirculating aquaculture systems, biogas production from fish sludge and optimization of renewable energy systems. Prior to starting as a Ph.D. candidate, Gerard was employed as an Engineer/Assistant Professor at the Western Norway University of Applied Sciences (2014–2021).

**Leila Jafari** is a Ph.D. student at the department of Biotechnology and Food Science, Norwegian University of Science and Technology (NTNU) and an exchange student at the Western Norway University of Applied Sciences (2021–2025). She has a master's degree in Ocean Resources (MSOCEAN), with specialization in Aquaculture (2018–2020). Her research involves water quality management in Recirculating Aquaculture Systems focusing on the diurnal variations in metabolites production rate.

**David Lande-Sudall** is an Associate Professor in Ocean Engineering at the Western Norway University of Applied Sciences (HVL), Bergen in Norway. David started his current position after completing his Ph.D. on co-located offshore wind and tidal stream turbines from the University of Manchester, UK. His research is focused on ocean renewable energy and particularly experimental hydrodynamics within HVL's MarinLab towing tank facility. David leads the research group Wind, Water and Waves (W3) and is currently Principal Investigator on the Research Council of Norway funded project, HYDROMORE (324388).

**Norbert Lümmen** is a physicist with a diploma degree from Heinrich-Heine-University in Düsseldorf/Germany (2001) and a doctoral degree in physical chemistry from the University in Cologne/Germany (2004). He has been postdoc at the University of Cologne/Germany and University of Bergen/Norway before he started working as associate professor in energy technology at the Department of Mechanical and Marine Engineering at Bergen University College (since 2017 Western Norway University of Applied Sciences) in 2010. His main work fields are thermodynamics, hydrogen technology and simulation of different types of energy systems.